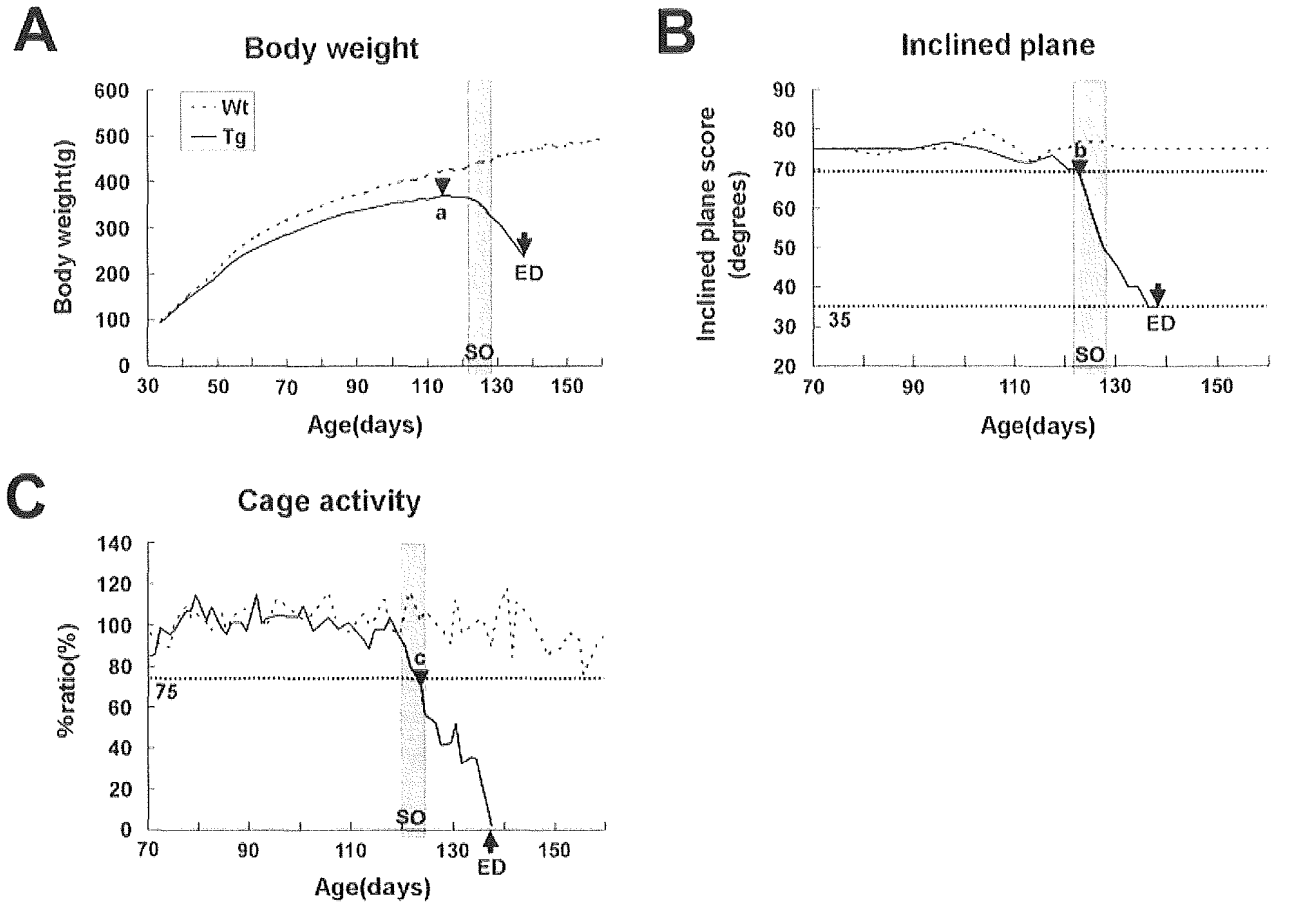

Fig. 4. Schematic presentation of the results from the body weight (**A**), inclined plane test (**B**), and cage activity (**C**) assessments. The onset defined by each measure (black arrowheads) and the end-stage of the disease (ED, black arrows) are indicated in the figures. a, pre-symptomatic onset: the day the transgenic rats scored their maximum body weight. b, muscle weakness onset: the earliest day the transgenic rats scored <70° in the inclined plane test. c, hypo-activity onset: the earliest day the transgenic rats scored <75% of the mean movements from 70–90 days of age in the cage activity measure. SO, subjective onset: the earliest day that observable functional deficits such as paralysis of the limbs or symptoms of general muscle weakness were observed subjectively in the open field (the gray shaded region in A–C).

60 days of age for all parameters (M1, M2, RG), however, even after the wild-type animals showed the decrease in their movement scores. The differences between the two groups increased markedly after 90 days of age for M1, M2, and RG (Fig. 3D–F). The performance of each rat fluctuated so markedly that the SCANET test seems to be inappropriate for statistical analysis.

Onset, End-Stage, and Duration of Disease in hSOD1 (G93A) Transgenic Rats

Using the quantitative analysis of disease progression by body-weight measurement, the inclined plane test, and cage activity, as described above, we defined three time points of "objective onset," as shown in Figure 4. The SCANET results did not allow us to define a time of objective onset, because we could not establish a stable baseline level using the data from the highly variable measurements we obtained, even for wild-type rats. The righting reflex failure was useful for detecting the time point of end-stage disease, which we defined as the generalized loss of motor activity in affected rats. A total of 20 transgenic rats assessed by body weight and the inclined plane test were analyzed for the day of objective onset, end-stage, and duration of the disease. The cage activity data from the eight transgenic rats were obtained simultaneously. The results are shown in Table IV.

The day the transgenic rats reached their maximum body weight was defined as pre-symptomatic onset (113.6 ± 4.8 days of age, black arrowhead in Fig. 4A, Table IV). This onset was judged retrospectively and always preceded the subjective onset (gray shaded region, Fig. 4A), which was determined by observable functional deficits in the open field, such as paralysis of limbs and symptoms of general muscle weakness. The

TABLE IV. Onset, End-Stage, and Duration in Days of Disease in hSOD1 (G93A) Transgenic Rats

Evaluation methods	Body weight and inclined plane (n = 20)	Cage activity (n = 8)
Objective onset		
Pre-symptomatic onset[a]	113.6 ± 4.8 (103–124)	
Muscle weakness onset[b]	125.2 ± 7.4 (110–144)	
Hypo-activity onset[c]		122.8 ± 9.2 (109–139)[c]
Subjective onset (SO)[d]	126.5 ± 7.1 (113–147)	121.3 ± 9.8 (109–140)
End-stage disease (ED)[e]	137.8 ± 7.1 (128–155)	134.1 ± 8.2 (122–149)
Duration[f]		
ED-a[g]	24.3 ± 6.5	
ED-b[h]	12.6 ± 3.5	
ED-c[i]		11.4 ± 1.3

Values are means ± SD.
[a] Maximum of body weight.
[b] Less than 70 degrees in the inclined plane test.
[c] Less than 75% in the mean movements of 70–90 days in the cage activity.
[d] Observable functional deficits.
[e] Righting reflex failure.
[f] Difference in days between ED and each onset;
[g] between ED and pre-symptomatic onset,
[h] between ED and muscle weakness onset,
[i] between ED and hypo-activity onset.

TABLE V. Comparison of the Onset, End-stage, and Duration in Days of Disease in the Forelimb-type and the Hindlimb-type Rats

	Forelimb type (n = 4)	Hindlimb type (n = 14)	General type* (n = 2)
Pre-symptomatic onset[a]	112.5 ± 6.7	114.6 ± 4.3	(108.5)
Muscle weakness onset[b]	125.8 ± 2.8	126.7 ± 7.3	(113.5)
End-stage disease (ED)[c]	134.0 ± 2.4	140.1 ± 7.1	(129.5)
Duration[d]			
ED-a[e]	21.5 ± 8.5	25.5 ± 6.2	(21)
ED-b[f]	8.3 ± 1.0	13.4 ± 3.0	(16)

Values are mean ± SD.
* Values of general-type rats are listed in parenthesis for reference.
[a] Maximum of body weight.
[b] Less than 70 degrees in the inclined plane test.
[c] Righting reflex failure.
[d] Difference in days between ED and each onset;
[e] between ED and pre-symptomatic onset,
[f] between ED and muscle weakness onset.

pre-symptomatic onset was the most sensitive of all the onset measures described in this study (Table IV).

The first day the transgenic rats scored <70° in the inclined plane test was defined as the muscle weakness onset (black arrowhead, Fig. 4B). We could judge this onset prospectively. Muscle weakness onset (125.2 ± 7.4 days of age, Table IV) was usually recorded before or at almost the same time as the subjective onset (8 days before to 1 day after, gray shaded region, Fig. 4B and 126.5 ± 7.1 days of age, Table IV). The day the transgenic rats scored 35° or less on the inclined plane test coincided with the day of righting reflex failure (black arrow, Fig. 4B).

The first day the transgenic rats scored <75% of their baseline movements in the cage activity test was defined as hypo-activity onset (black arrowhead, Fig. 4C and 122.8 ± 9.2 days of age, Table IV). We could also judge this onset prospectively. Hypo-activity onset was recorded 1 day before to 4 days after the subjective onset (SO, shown as the gray shaded region in Fig. 4C and 121.3 ± 9.8 days of age, Table IV). A 0% movement score for cage activity was seen at almost the same time as righting reflex failure (black arrow, Fig. 4C). Although disease onset and end-stage could be objectively defined with these methods, they had a wide range, of about 1 month, because of the diversity of the phenotypes (Table IV).

Differences in Disease Courses Between the Forelimb- and Hindlimb-Type Rats

Because we noticed variability in disease courses among different clinical types of hSOD1 (G93A) rats, we next assessed disease progression in 20 transgenic rats with forelimb- (n = 4), hindlimb- (n = 14), and general- (n = 2) type, using the probability of objective

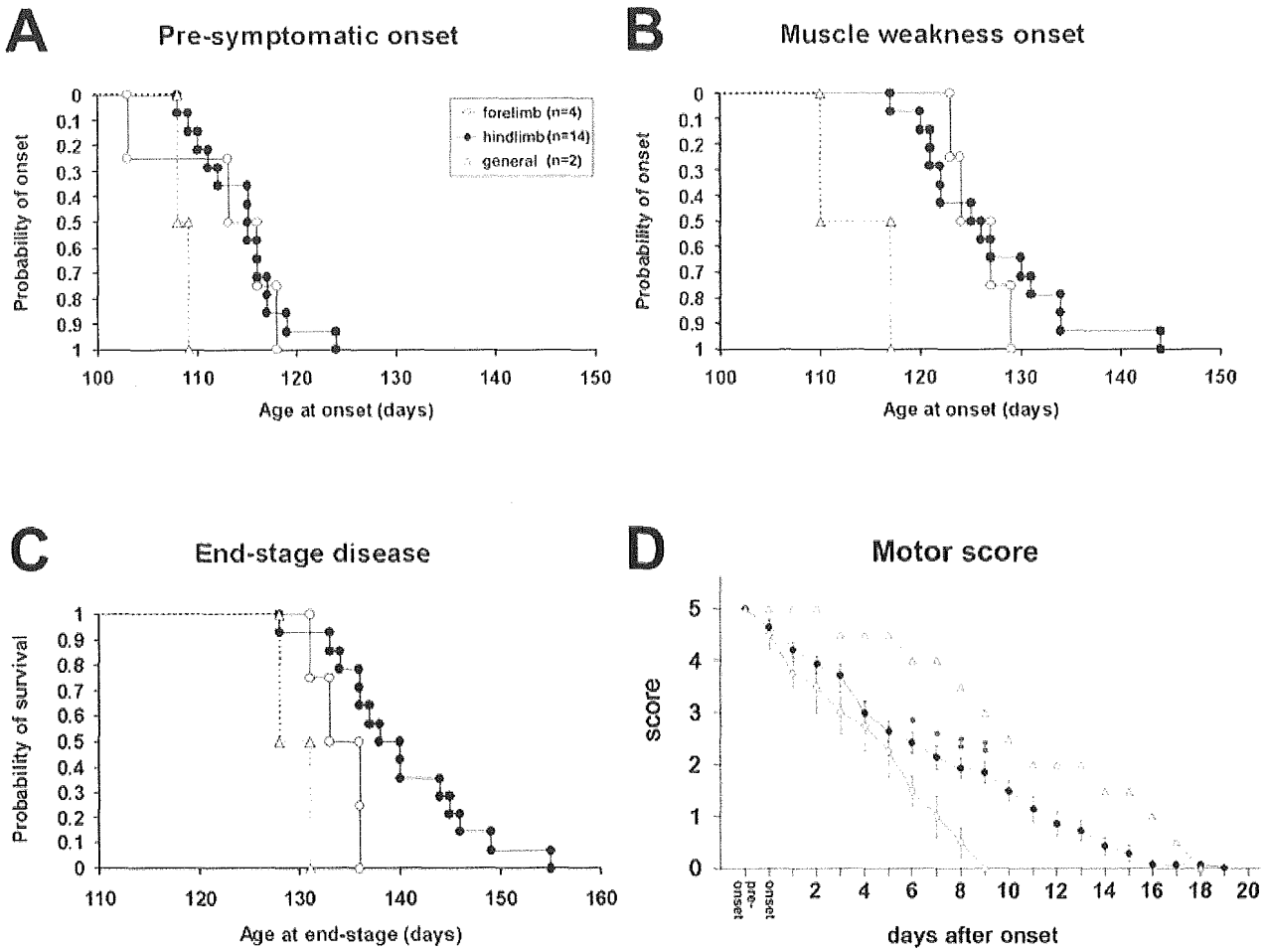

Fig. 5. Comparison of onset, end-stage, and disease progression in the forelimb-type ($n = 4$), and the hindlimb-type ($n = 14$) rats. Data from the general-type rats are also shown as dotted lines. **A,B:** The probability of the objective onsets. We did not see any differences in the probability of the objective onsets defined by body weight measurement (pre-symptomatic onset) and the inclined plane test (muscle weakness onset) between the forelimb- and hindlimb-type rats. **C:** The probability of survival as defined by end-stage disease. Survival was significantly shorter in the forelimb-type than in the hindlimb-type rats ($P < 0.05$, Log-rank test). **D:** Assessment of disease progression using the Motor score. Affected rats were evaluated after muscle weakness onset. The forelimb type worsened more quickly than the hindlimb type. Score decline correlated well with the exacerbation of symptoms in both clinical types, clearly and objectively. Bars = means ± SEM. Statistically significant differences between forelimb and hindlimb types are indicated in the figures. $*P < 0.05$. $**P < 0.01$; two-tailed unpaired Student's t-test.

onsets (pre-symptomatic onset and muscle weakness onset), the probability of survival defined by end-stage disease (failure in righting reflex), and the Motor score (Table V, Fig. 5). We did not see any differences in the objective onsets between the forelimb- and hindlimb-type rats (Fig. 5AB, Table V). However, survival as defined by end-stage disease was significantly shorter in the forelimb-type than in the hindlimb-type rats ($P < 0.05$, Log-rank test, Fig. 5C). Moreover, the duration of the disease calculated from the muscle weakness onset was also significantly shorter in the forelimb-type (8.3 ± 1.0 days) than in the hindlimb-type rats (13.4 ± 3.0 days) (see ED – b, $P < 0.01$, two-tailed unpaired Student's t-test, Table V).

The courses of functional deterioration evaluated by the Motor score after onset (muscle weakness onset) for each clinical type were well represented by the declines in their scores (Fig. 5D). The assessment by the Motor score also showed that disease progression in the forelimb type was more rapid than that in the hindlimb type (Fig. 5D).

Our results raise the question of why this variability in the disease course of each clinical type was observed. We speculated that there might be correlation between clinical type in G93A rats and the amount of locally expressed mutant hSOD1 (G93A) gene product. Therefore, we next investigated expression of the mutant hSOD1 gene in each segment of the spinal cord (cervical, thoracic, and lumbar) in the forelimb- and

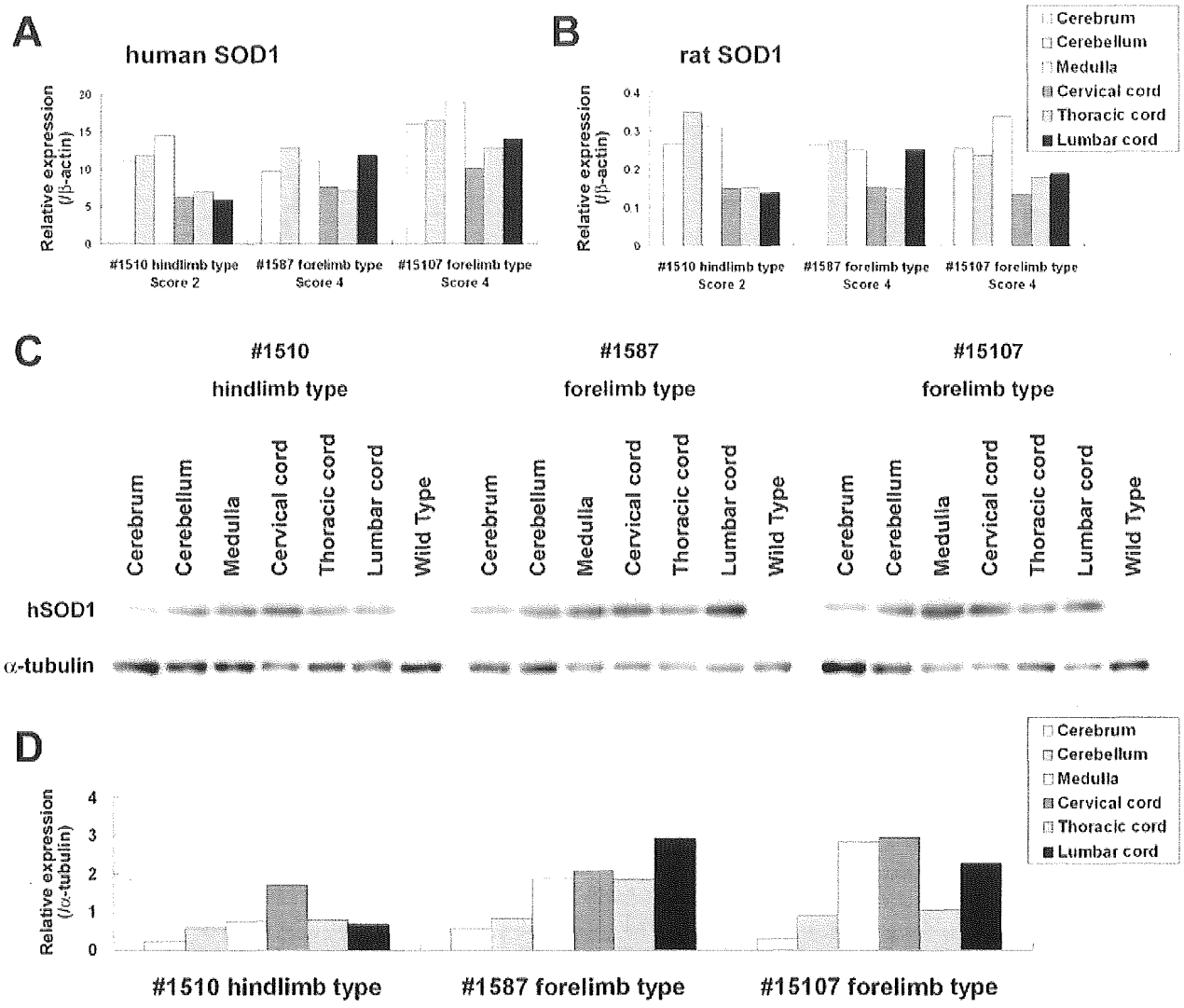

Fig. 6. The expression of mutant hSOD1 mRNA and protein in the cerebral cortex, cerebellum, medulla, and spinal cord (cervical, thoracic, and lumbar) of forelimb- and hindlimb-type rats. **A,B:** The amounts of human (A) and endogenous rat (B) SOD1 mRNA normalized to those of *β-actin* were quantified by real time RT-PCR analysis. **C,D:** Western blot analysis of the mutant hSOD1 protein was carried out in the same rats. Quantitative analysis was carried out with a Scion Image. The amounts of proteins were normalized to those of α-tubulin (D).

hindlimb-type rats by real time RT-PCR and Western blot analysis. However, at least at the stages after the apparent onset of muscle weakness, neither forelimb-type (#1587, Score 4 and #15107, Score 4) nor hindlimb-type rats (#1510, Score 2) necessarily expressed larger amounts of the mutant hSOD1 (G93A) transgene in the cervical cord or in the lumbar cord, respectively, at the mRNA and the protein level (Fig. 6). We also investigated the expression of endogenous rat SOD1 mRNA in the same rats by REAL TIME RT-PCR (Fig. 6B). Distribution of endogenous rat SOD1 mRNA expressed in each segment of the spinal cord showed almost the same pattern as that of mutant hSOD1 mRNA. The expression of endogenous rat SOD1 mRNA was lower than that of mutant hSOD1 mRNA. Thus, we could not detect any definite correlation between the hSOD1 (G93A) transgene local expression profile in the spinal cord and the phenotypes of G93A rats for either the forelimb-type or the hindlimb-type rats (Fig. 6).

Reduction in the Number of Spinal Cord Motor Neurons at Different Disease Stages

We examined histo-pathological changes in the spinal cords of the transgenic rats in comparison with those

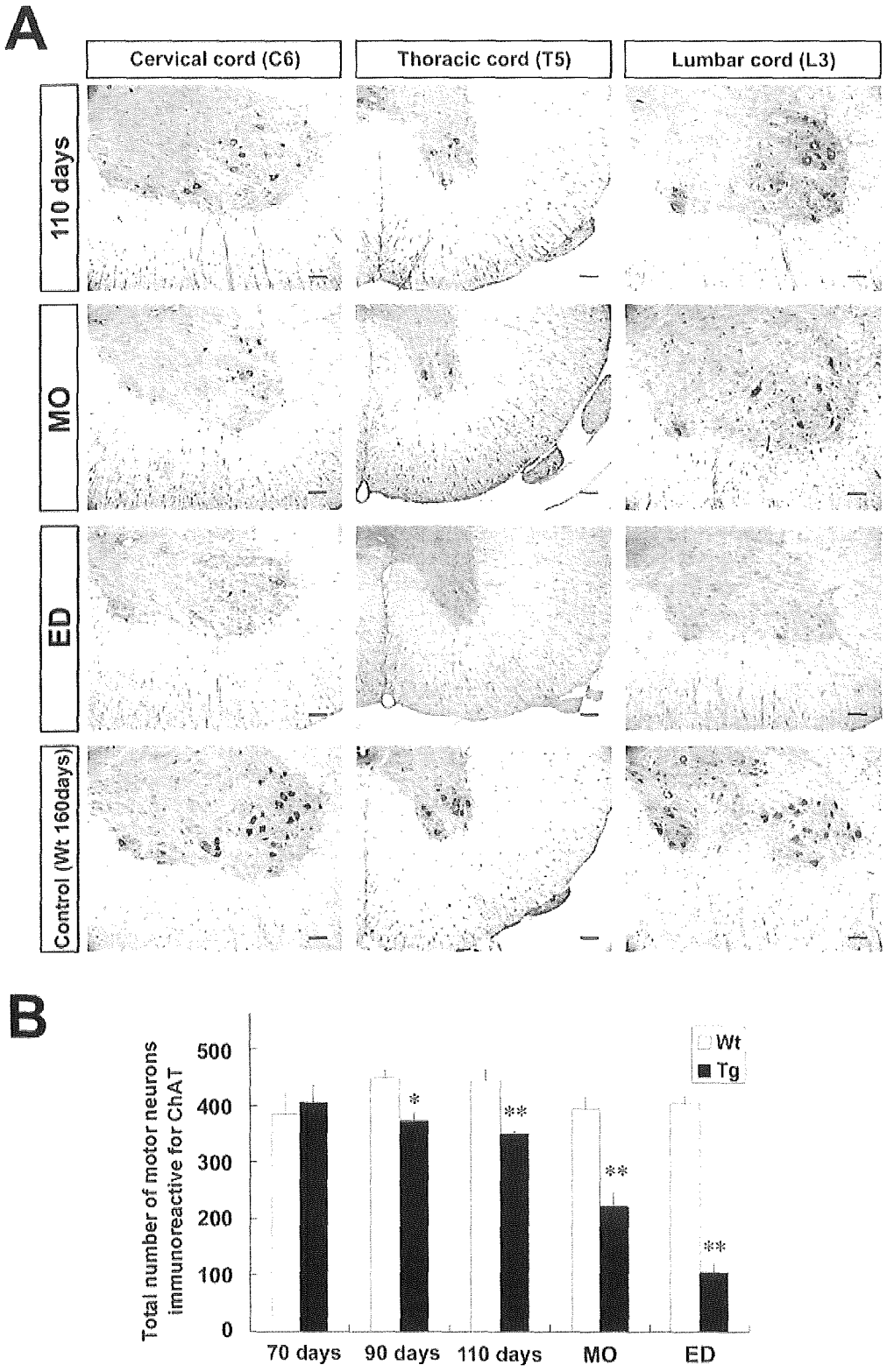

Fig. 7. The loss of motor neurons in the spinal cord of hSOD1 (G93A) transgenic rats at different stages. **A:** Immunohistochemical analysis of the spinal cord of transgenic rats. Transverse sections of the cervical (C6), thoracic (T5), and lumbar (L3) spinal cord of the transgenic rats and their wild-type littermates were stained with an anti-ChAT antibody to label viable motor neurons at the indicated stages (Scale bars = 100 μm). **B:** The number of ChAT immunoreactive motor neurons was counted and is shown in the histograms as the total number of motor neurons in the C6, T5, and L3 segments. This number began to decrease in the transgenic rats at 90 days of age, rapidly declined after 110 days of age, and fell to about 50% and 25% of wild-type rats at the muscle weakness onset (MO, around 125 days) and at end-stage disease (ED, around 140 days), respectively. Bars = means ± SEM ($n = 3$ for each genotype). *$P < 0.05$. **$P < 0.01$; two-tailed unpaired Student's t-test.

of their wild-type littermates at 70, 90, and 110 days of age, when the transgenic rats scored <70° in the inclined plane test (muscle weakness onset), and failed the righting reflex. To quantify the number of spinal motor neurons, we stained spinal cord sections of both groups with an anti-ChAT antibody.

As shown in Figure 7A, the numbers of ChAT immunoreactive motor neurons in the cervical (C6), thoracic (T5), and lumbar (L3) segments of the spinal cord decreased with disease progression. Quantitative analysis of the residual motor neurons showed that the total number of motor neurons in the transgenic rats began to decrease at 90 days of age, rapidly declined after 110 days of age, and fell to about 50% and 25% of the numbers in age-matched wild-type littermates at the time the score was <70° in the inclined plane test (muscle weakness onset) and of righting reflex failure, respectively (Fig. 7B).

DISCUSSION

Factors Underlying the Variability in Phenotypes of hSOD1 (G93A) Transgenic Rats

In previous studies of this G93A rat, only the hindlimb-type has been described, and the variety of phenotypes and variable clinical courses have not yet been mentioned (Nagai et al., 2001). Recently, however, another line of G93A rats backcrossed onto a Wistar background ($SOD1^{G93A/HWr}$ rats) was reported to present two phenotypes, including forelimb-type, and a large inter-litter variability in disease onset (Storkebaum et al., 2005). In the same way, commonly used FALS model mice harboring hSOD1 (G93A) gene have been reported to have clinical variability to some extent, and some of them dominantly show forelimb paralysis (Gurney et al., 1994). In this study, we recognized various clinical types, including forelimb-, hindlimb-, and general-type and established quantitative methods to evaluate disease progression that can be applied to any of the clinical types of this ALS model. We have also shown the variability in disease progression to depend on clinical types, that is, disease progression after the onset was faster in forelimb-type than in hindlimb-type rats. This difference may be due to the aggressiveness of the disease per se because we evaluated the time point of "death" (end-stage disease) according to righting reflex failure (Howland et al., 2002) to exclude the influence of feeding problems (bulbar region) and respiratory failure (level C2–C4).

These findings give rise to the next question; why is this variety of phenotypes and variability in the clinical course observed in the same transgenic line? There are at least three possible explanations. One is that the variation is due to the heterogeneous genetic background of the Sprague-Dawley (SD) rat (i.e., the strain used to generate this transgenic line), which might have led to different phenotypes. This idea is supported by the fact that the SD strain shows a large inter-individual disease variability in other models of neurodegenerative disorders, such as Huntington's disease (Ouary et al., 2000). Similar phenotypic variability takes place in human FALS carrying the same mutations in hSOD1 gene (Abe et al., 1996; Watanabe et al., 1997; Kato et al., 2001), which could be explained by heterogeneous genetic backgrounds. Thus, the present transgenic ALS model rats may be highly useful to understand the mechanisms of bulbar onset, arm onset, or leg onset that are seen in human disease. There may be modifier genes of these phenotypes, which should be identified in the future study.

TABLE VI. Adequacy of Evaluation Methods in Regard to Practical Use*

	Body weight	Inclined plane	Cage activity	SCANET	Motor score
Objectivity	A	B	A	A	B
Sensitivity	A	B	C	(A)	-
Specificity	C	B	C	C	A
Motivation independence	A	B	B	D	B
Skill requirements	A	B	A	A	B
Cost of apparatus	B	B	D	D	A

*A, more appropriate; B, appropriate; C, less appropriate; D, inappropriate.

The second is that there is variability in the expression of the mutant hSOD1 protein. The transcriptional regulation of this exogenous gene could be affected by one or more unknown factors, such as epigenetic regulation, and may not be expressed uniformly throughout the spinal cord of each animal. Therefore, some rats might express mutant proteins more in the cervical spinal cord and others might express more in the lumber cord, possibly resulting in the forelimb type and hindlimb type, respectively. However, we found no definite correlation between local expression levels of the mutant hSOD1 mRNA/protein in the spinal cord and the phenotypes of these animals, using real time RT-PCR and western blot analysis after the onset of muscle weakness, when the clinical type of the transgenic rats could be defined (Fig. 6). Moreover, the pathological analysis showed no correlation between the number of residual motor neurons in each segment and the phenotypes of end-stage animals. However, because >50% of spinal motor neurons have already degenerated at the stage of muscle weakness onset, whether local expression of the mutant hSOD1 gene and segmental loss of motor neurons correlate with the clinical types of G93A rats should be further investigated by analyzing younger animals at a stage when motor neuron loss has not progressed as much.

The third explanation involves a structural property of the mutant hSOD1 (G93A) protein itself. It is now thought that mutations in the hSOD1 gene may alter the 3-D conformation of the enzyme and, in turn, result in the SOD1 protein acquiring toxic properties that cause ALS (Deng et al., 1993; Hand and Rouleau 2002). For instance, the hSOD1 (G93A) mutant protein has been reported to be susceptible to nonnative protein–protein interactions because of its mutation site and unfolded structure (Shipp et al., 2003; Furukawa and

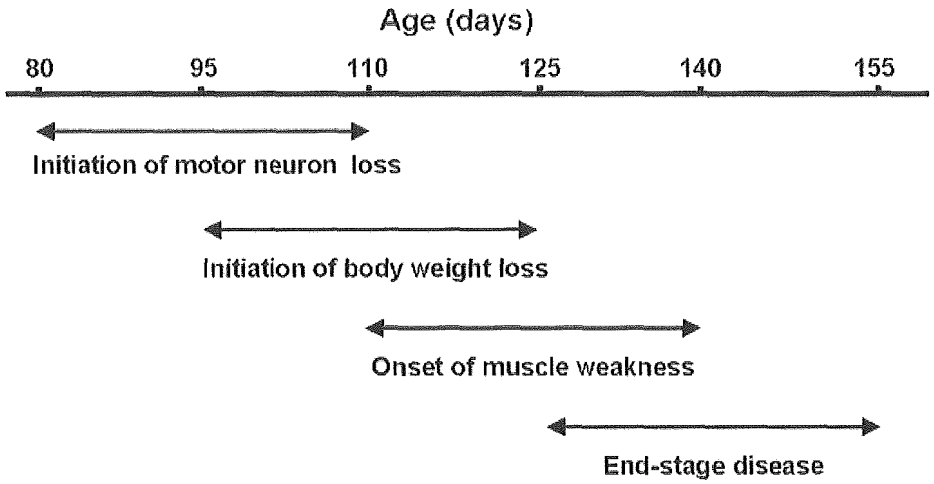

Fig. 8. Four stages of disease progression in hSOD1 (G93A) transgenic rats. The disease progression can be classified into four stages as shown. The range for each stage is about 1 month and overlaps approximately 2 weeks with the next stage.

O'Halloran, 2005), suggesting that the G93A mutation might accelerate the formation of SOD1 protein aggregates, which may ultimately sequester heat-shock proteins and molecular chaperones, disturb axonal transport or protein degradation machineries, including the ubiquitin-proteasome system (Borchelt et al., 1998; Bruening et al., 1999; Williamson and Cleveland 1999; Okado-Matsumoto and Fridovich 2002; Urushitani et al., 2002). Curiously, the mutated hSOD1 (G93A) protein is more susceptible to degradation by the ubiquitin-proteasome system and has a shorter half-life than other mutants (Fujiwara et al., 2005), suggesting that it may cause more unstable toxic aggregates in the spinal cord than other mutations. The degradation rate is also affected by environmental factors unique to each animal, such as the progressive decline of proteasome function with age (Keller et al., 2000), and these factors could contribute to the variability of the clinical course of G93A rats.

Taking all these findings into consideration, the mutated hSOD1 (G93A) protein may gain properties that are responsible for a variety of phenotypes and variability in the clinical course of the affected animals.

Characteristics of Different Methods for Assessing hSOD1 (G93A) Transgenic Rats

The ideal measure is not influenced by the judgment of the observer, sensitive to small abnormalities, specific to detect pathologic events that are related to pathogenesis of the ALS-like disease, not influenced by the motivational factors of rats, minimal in the requirements for skill in the observer, and inexpensive to carry out. We assessed each evaluation method by the categories in regard to practical use as shown in the Table 6.

The initiation of body weight loss seems to be an excellent marker to detect the onset and should be highly recommended. Muscle volume might have already started to decrease, even in the period of continuous weight gain, as reported for hSOD1 (G93A) transgenic mice (Brooks et al., 2004). As a result, it could detect an abnormality relatively earlier than subjective onset. The inclined plane test is considered to be the least defective method of all. It could objectively and specifically detect the decline in the muscle strength of these ALS model rats as a muscle weakness onset almost at the same time of the subjective onset. The cage activity measurement and SCANET require very expensive apparatus, and are limited by the availability of funds and space for making the measurements. Although SCANET test was most sensitive among these measures, it seems inappropriate for the statistical analysis, and does not add any more information than that obtained through simple observation of the rats because the performances of the rats might be severely affected by the extent of their motivation to explore. Motor score can specifically assess disease progression of each clinical type and is valuable in keeping the experimental costs at a minimum.

Correlation Between the Loss of Spinal Motor Neurons and Disease Stages

This study clearly shows the variable clinical course of G93A rats. According to our behavioral and histological analyses, we can divide the disease course of this transgenic model into four stages, whose durations have a range of about 1 month, as shown in Figure 8. Furthermore, we have established the pathological validity of the performance deficits detected by each measure of disease progression. "Initiation of motor neuron loss" was defined as a statistically significant decrease in the number of spinal motor neurons, which was found at around 90 days of age, but not 70 days of age (Fig. 7B). This coincides with, and seems to be sensitively detected by the marked difference in SCANET scores that begins at around 90 days of age (Fig. 3D–F). The "initiation of body weight loss" was usually detected at around 110 days of age as the peak body weight (pre-symptomatic onset, 113.6 ± 4.8 days of age, range = 103–124, Table IV). This stage coincides with the initiation of a rapid decline in the number of motor neurons at around 110 days of age (Fig. 7B). "Onset of muscle weakness" was detected at around 125 days of age, as assessed by the

inclined plane test (muscle weakness onset, 125.2 ± 7.4 days of age, range = 110–144, Table IV). This coincides with the number of spinal motor neurons in the transgenic rats being reduced to about 50% of the number in wild-type rats (Fig. 7B). We presume that transgenic rats do not present obvious muscle weakness until the number of motor neurons has been reduced to approximately half the number found in the healthy state. "End-stage disease" as defined by righting reflex failure was recorded at around 140 days of age (137.8 ± 7.1 days of age, range = 122–155, Table IV). At this stage, the affected rats had only about 25% of the spinal motor neurons of age- and gender-matched wild-type rats (Fig. 7B), and showed a generalized loss of motor activity. Thus, our findings allow us to estimate the extent of spinal motor neuron loss by evaluating the disease stage with the measures described in this study.

In summary, we have described the variable phenotypes of mutant hSOD1 (G93A) transgenic rats and established an evaluation system applicable to all clinical types of these rats. Disease stages defined by this evaluation system correlated well pathologically with the reduction of motor neurons. Our evaluation system of this animal model should be a valuable tool for future preclinical experiments aimed at developing novel treatments for ALS.

ACKNOWLEDGMENTS

We thank Dr. H.-N. Dai of the Department of Neuroscience, Georgetown University School of Medicine for technical advice and valuable discussions, and Dr. T. Yoshizaki and Miss K. Kaneko for participating in the assessment of transgenic rats with the Motor score. This work was supported by grants from CREST, Japan Society for the Promotion of Science to H.O., a Research Grant on Measures for Intractable Diseases from the Japanese Ministry of Health, Labour and Welfare to H.O., M.A., G.S. and Y.I., and a Grant-in-Aid for the 21st century COE program to Keio University from the Japanese Ministry of Education, Culture, Sports, Science and Technology.

REFERENCES

Abe K, Aoki M, Ikeda M, Watanabe M, Hirai S, Itoyama Y. 1996. Clinical characteristics of familial amyotrophic lateral sclerosis with Cu/Zn superoxide dismutase gene mutations. J Neurol Sci 136:108–116.

Azzouz M, Ralph GS, Storkebaum E, Walmsley LE, Mitrophanous KA, Kingsman SM, Carmeliet P, Mazarakis ND. 2004. VEGF delivery with retrogradely transported lentivector prolongs survival in a mouse ALS model. Nature 429:413–417.

Barneoud P, Lolivier J, Sanger DJ, Scatton B, Moser P. 1997. Quantitative motor assessment in FALS mice: a longitudinal study. Neuroreport 8:2861–2865.

Borchelt DR, Wong PC, Becher MW, Pardo CA, Lee MK, Xu ZS, Thinakaran G, Jenkins NA, Copeland NG, Sisodia SS, Cleveland DW, Price DL, Hoffman PN. 1998. Axonal transport of mutant superoxide dismutase 1 and focal axonal abnormalities in the proximal axons of transgenic mice. Neurobiol Dis 5:27–35.

Brooks KJ, Hill MD, Hockings PD, Reid DG. 2004. MRI detects early hindlimb muscle atrophy in Gly93Ala superoxide dismutase-1 (G93A SOD1) transgenic mice, an animal model of familial amyotrophic lateral sclerosis. NMR Biomed 17:28–32.

Brown RH Jr. 1995. Amyotrophic lateral sclerosis: recent insights from genetics and transgenic mice. Cell 80:687–692.

Bruening W, Roy J, Giasson B, Figlewicz DA, Mushynski WE, Durham HD. 1999. Up-regulation of protein chaperones preserves viability of cells expressing toxic Cu/Zn-superoxide dismutase mutants associated with amyotrophic lateral sclerosis. J Neurochem 72:693–699.

Chiu AY, Zhai P, Dal Canto MC, Peters TM, Kwon YW, Prattis SM, Gurney ME. 1995. Age-dependent penetrance of disease in a transgenic mouse model of familial amyotrophic lateral sclerosis. Mol Cell Neurosci 6:349–362.

de Belleroche J, Orrell R, King A. 1995. Familial amyotrophic lateral sclerosis/motor neurone disease (FALS): a review of current developments. J Med Genet 32:841–847.

Deng HX, Hentati A, Tainer JA, Iqbal Z, Cayabyab A, Hung WY, Getzoff ED, Hu P, Herzfeldt B, Roos RP, Warner C, Deng G, Soriano E, Smyth C, Parge HE, Ahmed A, Roses AD, Hallewell RA, Pericak-Vance MA, Siddique T. 1993. Amyotrophic lateral sclerosis and structural defects in Cu, Zn superoxide dismutase. Science 261:1047–1051.

Fujiwara N, Miyamoto Y, Ogasahara K, Takahashi M, Ikegami T, Takamiya R, Suzuki K, Taniguchi N. 2005. Different immunoreactivity against monoclonal antibodies between wild-type and mutant copper/zinc superoxide dismutase linked to amyotrophic lateral sclerosis. J Biol Chem 280:5061–5070.

Furukawa Y, O'Halloran TV. 2005. Amyotrophic lateral sclerosis mutations have the greatest destabilizing effect on the Apo- and reduced form of SOD1, leading to unfolding and oxidative aggregation. J Biol Chem 280:17266–17274.

Gale K, Kerasidis H, Wrathall JR. 1985. Spinal cord contusion in the rat: behavioral analysis of functional neurologic impairment. Exp Neurol 88:123–134.

Garbuzova-Davis S, Willing AE, Milliken M, Saporta S, Zigova T, Cahill DW, Sanberg PR. 2002. Positive effect of transplantation of hNT neurons (NTera 2/D1 cell-line) in a model of familial amyotrophic lateral sclerosis. Exp Neurol 174:169–180.

Gurney ME, Pu H, Chiu AY, Dal Canto MC, Polchow CY, Alexander DD, Caliendo J, Hentati A, Kwon YW, Deng HX, Chen W, Zhai F, Sufit RL, Siddique T. 1994. Motor neuron degeneration in mice that express a human Cu,Zn superoxide dismutase mutation. Science 264:1772–1775.

Hand CK, Rouleau GA. 2002. Familial amyotrophic lateral sclerosis. Muscle Nerve 25:135–159.

Howland DS, Liu J, She Y, Goad B, Maragakis NJ, Kim B, Erickson J, Kulik J, DeVito L, Psaltis G, DeGennaro LJ, Cleveland DW, Rothstein JD. 2002. Focal loss of the glutamate transporter EAAT2 in a transgenic rat model of SOD1 mutant-mediated amyotrophic lateral sclerosis (ALS). Proc Natl Acad Sci USA 99:1604–1609.

Inoue H, Tsukita K, Iwasato T, Suzuki Y, Tomioka M, Tateno M, Nagao M, Kawata A, Saido TC, Miura M, Misawa H, Itohara S, Takahashi R. 2003. The crucial role of caspase-9 in the disease progression of a transgenic ALS mouse model. EMBO J 22:6665–6674.

Kaspar BK, Llado J, Sherkat N, Rothstein JD, Gage FH. 2003. Retrograde viral delivery of IGF-1 prolongs survival in a mouse ALS model. Science 301:839–842.

Kato M, Aoki M, Ohta M, Nagai M, Ishizaki F, Nakamura S, Itoyama Y. 2001. Marked reduction of the Cu/Zn superoxide dismutase polypeptide in a case of familial amyotrophic lateral sclerosis with the homozygous mutation. Neurosci Lett 312:165–168.

Keller JN, Huang FF, Zhu H, Yu J, Ho YS, Kindy TS. 2000. Oxidative stress-associated impairment of proteasome activity during ischemia-reperfusion injury. J Cereb Blood Flow Metab 20:1467–1473.

Landis JR, Koch GG. 1977. The measurement of observer agreement for categorical data. Biometrics 33:159–174.

Mikami Y, Toda M, Watanabe M, Nakamura M, Toyama Y, Kawakami Y. 2002. A simple and reliable behavioral analysis of locomotor function after spinal cord injury in mice. Technical note. J Neurosurg Spine 97:142–147.

Mulder DW, Kurland LT, Offord KP, Beard CM. 1986. Familial adult motor neuron disease: amyotrophic lateral sclerosis. Neurology 36:511–517.

Nagai M, Aoki M, Miyoshi I, Kato M, Pasinelli P, Kasai N, Brown RH, Jr., Itoyama Y. 2001. Rats expressing human cytosolic copper-zinc superoxide dismutase transgenes with amyotrophic lateral sclerosis: associated mutations develop motor neuron disease. J Neurosci 21:9246–9254.

Ohki-Hamazaki H, Sakai Y, Kamata K, Ogura H, Okuyama S, Watase K, Yamada K, Wada K. 1999. Functional properties of two bombesin-like peptide receptors revealed by the analysis of mice lacking neuromedin B receptor. J Neurosci 19:948–954.

Okada Y, Shimazaki T, Sobue G, Okano H. 2004. Retinoic-acid-concentration-dependent acquisition of neural cell identity during in vitro differentiation of mouse embryonic stem cells. Dev Biol 275:124–142.

Okado-Matsumoto A, Fridovich I. 2002. Amyotrophic lateral sclerosis: a proposed mechanism. Proc Natl Acad Sci USA 99:9010–9014.

Ouary S, Bizat N, Altairac S, Menetrat H, Mittoux V, Conde F, Hantraye P, Brouillet E. 2000. Major strain differences in response to chronic systemic administration of the mitochondrial toxin 3-nitropropionic acid in rats: implications for neuroprotection studies. Neuroscience 97:521–530.

Rivlin AS, Tator CH. 1977. Objective clinical assessment of motor function after experimental spinal cord injury in the rat. J Neurosurg 47: 577–581.

Rosen DR, Siddique T, Patterson D, Figlewicz DA, Sapp P, Hentati A, Donaldson D, Goto J, O'Regan JP, Deng HX, Rahmani Z, Krizus A, McKenna-Yasek D, Cayabyab A, Gasten SM, Berger R, Tanzi RE, Halperin JJ, Herzfeldt B, van den Bergh R, Hung WY, Bird T, Deng G, Mulder DW, Smyth C, Laing NG, Soriano E, Pericak-Vance MA, Haines J, Reuleau GA, Gusella JS, Horvitz HR, Brown RH Jr. 1993. Mutations in Cu/Zn superoxide dismutase gene are associated with familial amyotrophic lateral sclerosis. Nature 362:59–62.

Shipp EL, Cantini F, Bertini I, Valentine JS, Banci L. 2003. Dynamic properties of the G93A mutant of copper-zinc superoxide dismutase as detected by NMR spectroscopy: implications for the pathology of familial amyotrophic lateral sclerosis. Biochemistry 42:1890–1899.

Storkebaum E, Lambrechts D, Dewerchin M, Moreno-Murciano MP, Appelmans S, Oh H, Van Damme P, Rutten B, Man WY, De Mol M, Wyns S, Manka D, Vermeulen K, Van Den Bosch L, Mertens N, Schmitz C, Robberecht W, Conway EM, Collen D, Moons L, Carmeliet P. 2005. Treatment of motoneuron degeneration by intracerebroventricular delivery of VEGF in a rat model of ALS. Nat Neurosci 8:85–92.

Sun W, Funakoshi H, Nakamura T. 2002. Overexpression of HGF retards disease progression and prolongs life span in a transgenic mouse model of ALS. J Neurosci 22:6537–6548.

Urushitani M, Kurisu J, Tsukita K, Takahashi R. 2002. Proteasomal inhibition by misfolded mutant superoxide dismutase 1 induces selective motor neuron death in familial amyotrophic lateral sclerosis. J Neurochem 83:1030–1042.

Wang LJ, Lu YY, Muramatsu S, Ikeguchi K, Fujimoto K, Okada T, Mizukami H, Matsushita T, Hanazono Y, Kume A, Nagatsu T, Ozawa K, Nakano I. 2002. Neuroprotective effects of glial cell line-derived neurotrophic factor mediated by an adeno-associated virus vector in a transgenic animal model of amyotrophic lateral sclerosis. J Neurosci 22: 6920–6928.

Watanabe M, Aoki M, Abe K, Shoji M, Iizuka T, Ikeda Y, Hirai S, Kurokawa K, Kato T, Sasaki H, Itoyama Y. 1997. A novel missense point mutation (S134N) of the Cu/Zn superoxide dismutase gene in a patient with familial motor neuron disease. Hum Mutat 9:69–71.

Weydt P, Hong SY, Kliot M, Moller T. 2003. Assessing disease onset and progression in the SOD1 mouse model of ALS. Neuroreport 14: 1051–1054.

Williamson TL, Cleveland DW. 1999. Slowing of axonal transport is a very early event in the toxicity of ALS-linked SOD1 mutants to motor neurons. Nat Neurosci 2:50–56.

Neuropathology 2005; **25**, 365–370

Workshop: Recent Advances in Motor Neuron Disease

Development of a rat model of amyotrophic lateral sclerosis expressing a human *SOD1* transgene

Masashi Aoki,[1] Shinsuke Kato,[2] Makiko Nagai[1] and Yasuto Itoyama[1]

[1]Department of Neurology, Tohoku University School of Medicine, Sendai, and [2]Department of Neuropathology, Institute of Neurological Sciences, Faculty of Medicine, Tottori University, Yonago, Japan

Mutations in copper–zinc superoxide dismutase gene (*SOD1*) have been linked to some familial cases of ALS. We report here that rats that express a human *SOD1* transgene with two different ALS-associated mutations (G93A and H46R) develop striking motor neuron degeneration and paralysis. By comparing the two transgenic rats with different *SOD1* mutations, we demonstrate that the time course in these rats was similar to human *SOD1*-mediated familial ALS. As in the human disease and transgenic ALS mice, pathological analysis shows selective loss of motor neurons in the spinal cords of these transgenic rats. In addition, typical neuronal Lewy body-like hyaline inclusions as well as astrocytic hyaline inclusions identical to those in human familial ALS are observed in the spinal cords. The larger size of this rat model as compared with the ALS mice will facilitate studies involving manipulations of spinal fluid (implantation of intrathecal catheters for chronic therapeutic studies; CSF sampling) and spinal cord (e.g., direct administration of viral- and cell-mediated therapies).

Key words: astrocytic hyaline inclusions, amyotrophic lateral sclerosis, Lewy body-like hyaline inclusions, mutation, rat, *SOD1*, transgenic.

INTRODUCTION

ALS is a fatal neurodegenerative disease caused by the selective death of motor neurons.[1] Approximately 10% of the cases of ALS are inherited, usually as an autosomal dominant trait. In 25% of familial cases, the disease is caused by mutations in the gene encoding cytosolic copper–zinc superoxide dismutase (*SOD1*).[2,3] Nearly 100 different mutations in the *SOD1* gene have been identified in familial ALS.[4] Why the mutations cause motor neuron degeneration has not been fully elucidated.

In familial ALS kindred with mutations in the *SOD1* gene, the age of onset of weakness varies greatly but the duration of illness appears to be characteristic to each mutation. For example, in patients with the L84V mutation, the average life expectancy is less than 1.5 years after the onset of symptoms,[5,6] whereas patients harboring the H46R mutation have an average life expectancy of 18 years after the disease onset.[2,7] In view of the evidence supporting the idea that familial ALS variants of *SOD1* enzymes acquire toxic properties, the variations in the duration of illness in different kindred might arise because each mutation imparts different degrees of toxicity to the mutant protein.[8]

To date, several *SOD1* mutants of transgenic mice have been generated.[9–12] These mice exhibit the ALS-like clinical features and have importantly advanced our understanding of the pathogenesis of neuronal cell death induced by mutant SOD1 protein. They have also facilitated therapeutic trials. However, some types of experimental manipulations have been difficult in the ALS mice because of their innate size limitations. It has been almost impossible, for example, to analyze CSF from the ALS mice, even at single time points. It has also been very difficult to use therapies that involve administration of compounds into the CSF. There is only a single report of pump-mediated delivery of therapies to the CSF of the ALS mice, and that approach was intraventricular rather than intrathecal;[13] it is likely that intrathecal administration will produce significantly better therapeutic levels of compounds at the spinal cord level than will the intraventricular approach.[14] It has also been difficult to obtain sufficient tissue to perform extensive biochemical analyzes, such as investigations of post-transcriptional modifications of proteins like SOD1 itself during disease progression. For these reasons and in order

Correspondence: Masashi Aoki MD, PhD, Department of Neurology, Tohoku University School of Medicine, Seiryo-machi, Sendai 980-8574, Japan. Email: aokim@mail.tains.tohoku.ac.jp

Received 1 December 2004; accepted 8 December 2004.

to reproduce the different degrees of toxicity to the mutant protein by mutations, we have developed a rat model of ALS by expressing a human *SOD1* transgene with two ALS-associated mutations: H46R and G93A.[15]

CONSTRUCTION OF TRANSGENIC MICE EXPRESSING MUTANT HUMAN *SOD1*

We elected to make transgenic rats with two mutations in the *SOD1* genes: histidine 46 to arginine (H46R) and glycine 93 to alanine (G93A). In patients we have encountered with these mutations, the phenotypes are quite different. For H46R patients, progression is extremely slow[2,7] whereas patients with the $SOD1^{G93A}$ mutation demonstrate a more fulminant, classical clinical course.[16] Moreover, the transgenic ALS mouse with this G93A mutation has been widely distributed and studied throughout the world.[9]

To generate the transgenic rats with the H46R and the G93A mutations, we first obtained human genomic PAC clones encompassing the entire human *SOD1* gene; we then subcloned this gene within an 11.5 kb *Eco*RI–*Bam*HI fragment. Site-directed mutagenesis was used to generate clones with either the H46R or the G93A mutations. The mutated 11.5 kb *Eco*RI–*Bam*HI fragments were microinjected into fertilized eggs from Sprague Dawley (SD) rats (Japan SLC, Hamamatsu, Japan). Twenty-five potential transgenic H46R pups were obtained. From these, five founders with the H46R mutant transgene were identified using PCR and Southern blotting. Fifty-two potential transgenic G93A pups were obtained. From these, seven founders with the G93A mutant transgene were identified. Levels of accumulated mutant *SOD1* were measured for almost all founders by quantitative protein immunoblotting of spinal cord extracts using antibody against a peptide sequence that is identical in human and rat *SOD1*.

The transgenic rats expressing the higher levels of each human *SOD1* mutant (lines G93A-39 and H46R-4) have developed motor neuron disease (Fig. 1). Clinically apparent weakness, denoted by dragging of one hindlimb without limb tremor, was evident somewhat later. The mean age of onset of this clinical weakness for the G93A-39 line was 122.9 days ($n = 14$); for the H46R-4 line, the age of onset was 171.7 days ($n = 11$) (Fig. 1). Simultaneously with the onset of clinical weakness, the affected rats showed prominent weight loss. Although the initial clinical manifestation of weakness was unilateral leg paralysis, this progressed and became bilateral in both lines of rats. In the early stages of the illness, another distinctive abnormality was increased tone in the tail musculature, resulting in an elevated, segmentally spastic tail posture. As the disease progressed, the rats exhibited marked muscle wasting in the hindlimbs, typically dragging themselves about the

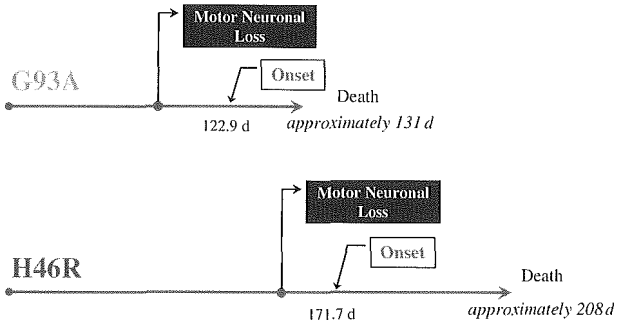

Fig. 1 Progression of mutant superoxide dismutase-mediated disease. From the presymptomatic stage, the anterior horns of the same rats revealed decreased numbers of large, multipolar neuronal cells (motor neurons) with proliferation of small non-neuronal cells with morphological characteristics of astrocytes and microglia. The ages of onset and death for the G93A-39 and H46R-4 rats are indicated.

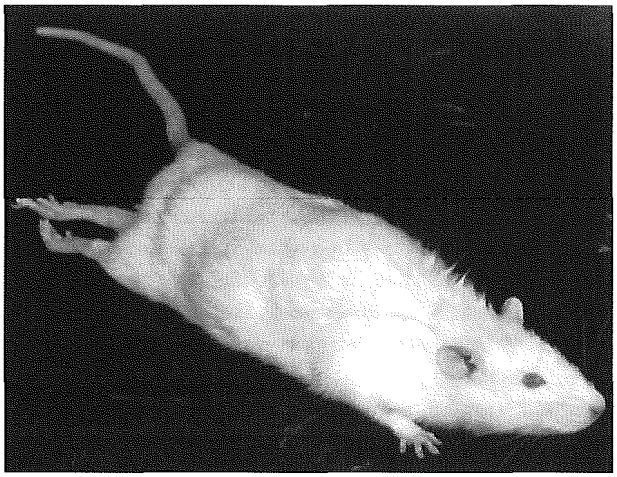

Fig. 2 An affected transgenic rat from the H46R-4 line demonstrates hindlimb weakness and abnormal posturing with segmental spasticity of the tail.

cage using the forelimbs (Fig. 2). Thereafter, the forelimbs also became weak, in association with further weight loss. At end-stage, the affected rats could not drink water and died. The mean duration of the disease in the G93A-39 and H46R-4 lines were 8.3 days ($n = 14$) and 37.2 days ($n = 11$), respectively. All rats were handled according to approved animal protocols in our institution.

HISTOPATHOLOGICAL AND IMMUNOHISTOCHEMICAL ANALYZES

The H46R and G93A transgenic rats exihibit the same histopathological changes as those in human familial ALS patients with *SOD1* gene mutations. Therefore, at present,

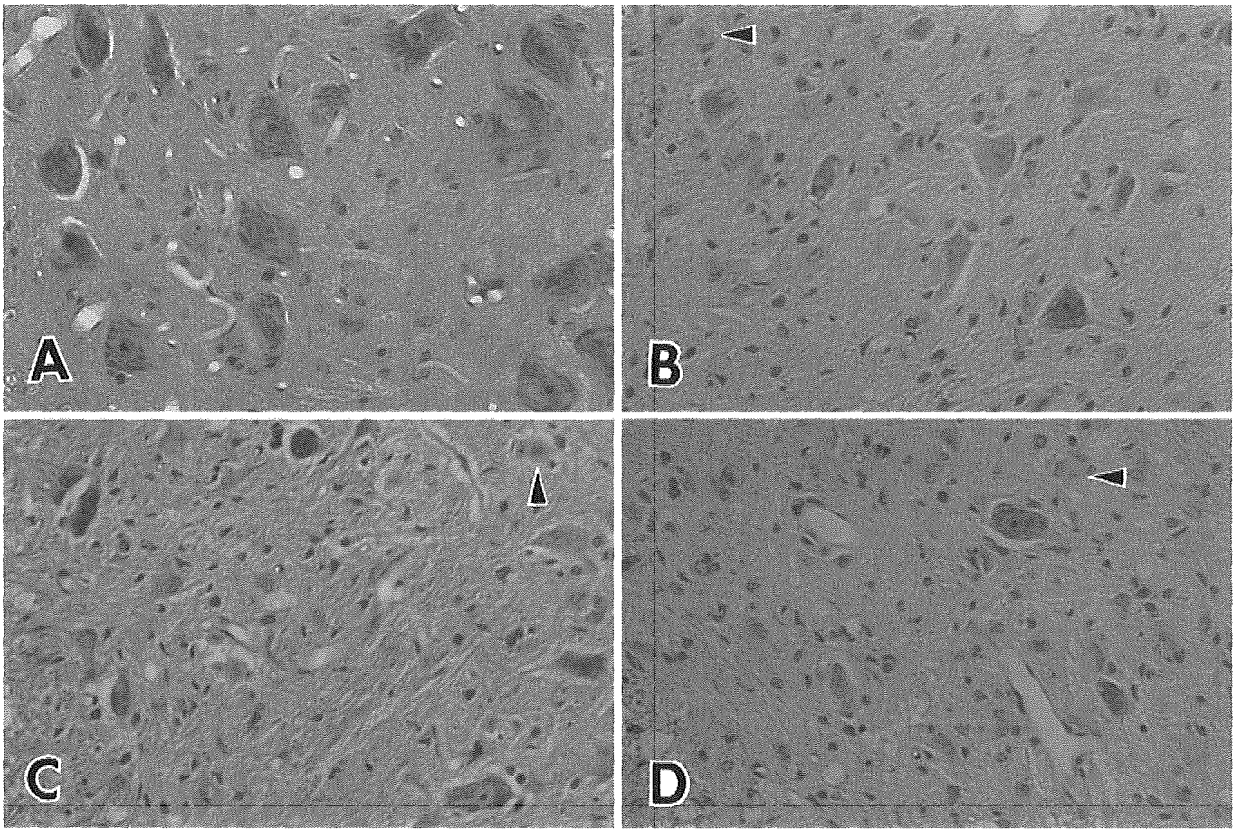

Fig. 3 Histological and histopathological findings in H46R transgenic rats and littermate. (A) The anterior horn of the spinal cord in littermate rat at the age of 160 days: approximately 15 normal anterior horn cells can be observed. (B) The anterior horn of the spinal cord in H46R transgenic rat at the age of 160 days: approximately six anterior horn cells can be counted in the H46R transgenic rat of this age, that is, the number of the anterior horn cells is decreased with astrocytic gliosis, histopathologically, in comparison with the littermate at the same age in (A). A core and halo-type astrocytic hyaline inclusion (Ast-HI) is evident (arrowhead). (C) The anterior horn of the spinal cord in the H46R transgenic rat at the age of 170 days: the histopathological finding of this age reveals loss of the anterior horn cells and gliosis of the spinal cords. A core and halo-type Ast-HI can be observed (arrowhead). (D) The anterior horn of the spinal cord in the H46R transgenic rat at the age of 200 days corresponding to the end-stage: approximately two anterior horn cells can be recognized at this terminal stage; the H46R rats of the terminal stage show severe loss of the anterior horn cells with gliosis of the spinal cords histopathologically compatible with those in ALS patients with clinical courses of over 5 years. A core and halo-type Ast-HI can be seen (arrowhead). As in human ALS patients, small-sized remaining anterior horn cells that appear to be normal are also observed throughout the disease courses in H46R transgenic rats (B–D) ((A–D): HE; magnification: ×400).

we think that the H46R and G93A transgenic rats are neuropathologically most optimal as animal models of familial ALS with the *SOD1* mutations. An essential histopathological finding of the spinal cords in ALS patients is loss of the anterior horn cells.[17] When we focus on the anterior horn cells of the spinal cords in both H46R and G93A transgenic rats, the anterior horn cells of the H46R and G93A transgenic rats are decreased before the development of clinical motor deficits. At the level of cellular pathology, the H46R and G93A transgenic rats develop Lewy body-like hyaline inclusions (LBHI) in neurons and astrocytes, which are morphological hallmarks of certain human familial ALS patients with the *SOD1* gene mutations.[17–20]

With respect to the histopathological aspects of H46R transgenic rats, the number of the anterior horn cells of the 160-day-old H46R rats that exhibit hind limb paresis is decreased with astrocytic gliosis in the spinal cords in comparison with the littermates at the same age (Fig. 3A,B). At 170 days of age when the H46R rats indicate hindlimb paraplegia sometimes associated with forelimb weakness, the histopathological finding of this clinical stage reveals more severe loss of the anterior horn cells and gliosis of the spinal cords in comparison with that of 160 days of age (Fig. 3B,C). At 200 days of age corresponding to the end-stage when the H46R rats clinically display quadriplegia or a moribund state, the H46R rats of this end-stage show severe loss of the anterior horn cells with gliosis of the spi-

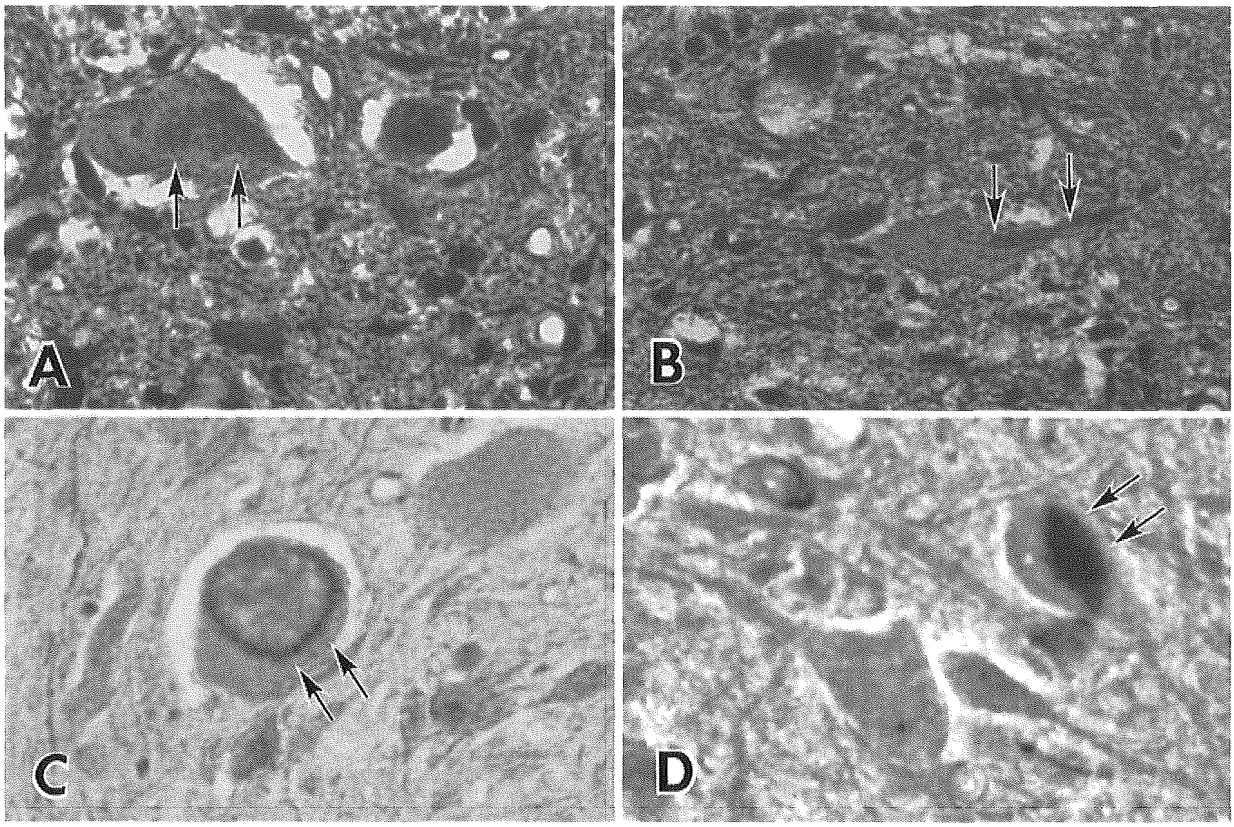

Fig. 4 Neuronal Lewy body-like hyaline inclusions (LBHI) in H46R transgenic rats. (A) A typical intracytoplasmic neuronal LBHI with a core and halo is indicated by double arrows (HE; magnification: ×820). (B) A neuronal LBHI with a core and halo is located from the cytoplasm to the dendrite (double arrows) (HE; magnification: ×820). (C) An intracytoplasmic LBHI is positive for SOD1; only the periphery of the neuronal LBHI is strongly immunostained (double arrows) (Immunostaining for SOD1; magnification: ×820). (D) An intracytoplasmic LBHI is diffusely immunostained (double arrows) (Immunostaining for SOD1; magnification: ×820). (Figure 4C is from Kato *et al.*[18] and reproduced with permission from *Acta Neuropathol*).

nal cords histopathologically compatible with those in ALS patients with clinical courses of over 5 years (Fig. 3D). As in human ALS patients, small-sized remaining anterior horn cells that appear to be normal in HE preparations are also observed throughout the disease courses in H46R and G93A transgenic rats (Fig. 3A–D).

As for the cell-pathological and immunohistochemical aspects, the rodent familial ALS model of these rats has the other important cellular pathological finding compatible with that in human familial ALS patients with the *SOD1* gene mutations; typical intracytoplasmic neuronal LBHI are observed in the remaining anterior horn cells of the spinal cords in the rat model of familial ALS. Cell-pathologically, the intracytoplasmic neuronal LBHI in the rat model of ALS are identical to those in human familial ALS. In both the rat model and human familial ALS, neuronal LBHI are formed not only in the cytoplasm but also in dendrites (Fig. 4A,B). Immunohistochemically, as in human mutant *SOD1*-mediated familial ALS,[17,19,20] the neuronal LBHI in the rat model of ALS with the H46R and G93A are positive for SOD1 (Fig. 4C,D). The reaction product deposits of the antibody against SOD1 are generally restricted to the periphery of the LBHI that show eosinophilic cores with palor peripheral halos in HE preparations (Fig. 4C). The immunostaining in intracytoplasmic and intradendtritic ill-defind LBHI is distributed throughout each of the inclusions (Fig. 4D). The rat model of ALS with the H46R and G93A also develops astrocytic hyaline inclusions (Ast-HI) that are identical structures observed in human long-term surviving familial ALS patients with the *SOD1* gene mutation.[17,19,20] In HE preparations, similarly in neuronal LBHI, Ast-HI are eosinophilic (Fig. 5A) or slightly pale inclusions and sometimes show an eosinophilic core with palor peripheral halos (Fig. 3B–D). The Ast-HI are generally round to oval and sometimes sausage-like in shape. As in neuronal LBHI, immunohistochemically, Ast-HI are intensely immunostained by the antibody against SOD1 (Fig. 5B).

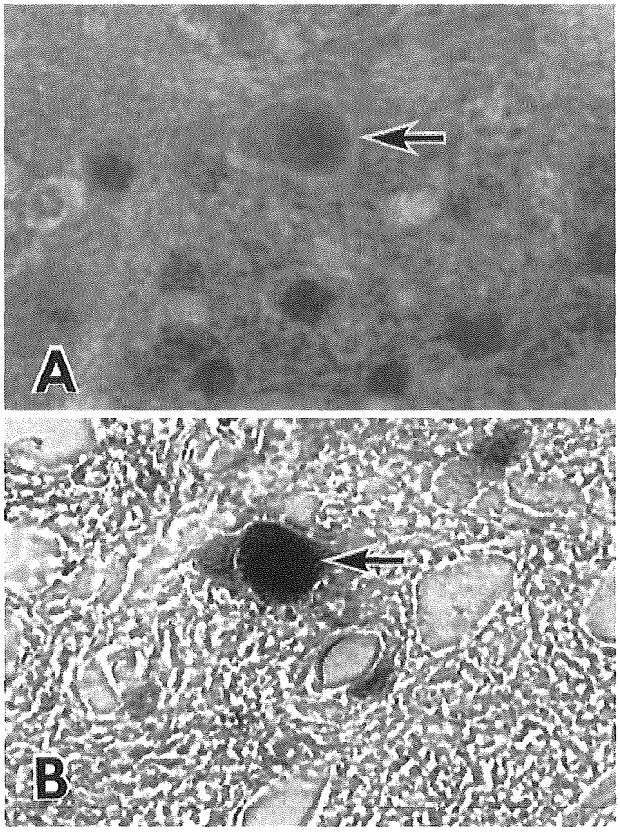

Fig. 5 Astrocytic hyaline inclusions (Ast-HI) in H46R transgenic rats. (A) Typical eosinophilic Ast-HI can be seen (arrow) (HE; magnification: ×1200). (B) An Ast-HI is strongly positive for SOD1 (arrow) (Immunostaining for SOD1; magnification: ×1200).

DISCUSSION

We have established lines of rats that express transgenes for mutant SOD1 protein with two different ALS-associated mutations: H46R and G93A. Rats with the highest transgene copy numbers and levels of expression of the mutant protein develop a paralytic disorder characterized by fulminant motor neuron death accompanied by astrogliosis and microgliosis. Particularly striking in our data is not only the earlier onset of the G93A disease but also the much more rapid course in the G93A-39 (8 days) as compared to the H46R-4 (37 days) rats. We do not understand the basis for this difference in rate of disease progression, but we note those factors determining the time course in these rats are likely to be relevant to human mutant *SOD1*-mediated familial ALS. The human H46R cases also progress very slowly, with a mean survival of 16.8 ± 6.8 years.[2,7] By contrast, the mean survival of the G93A cases in one report was 2.2 ± 1.5 years.[16] Although it is tempting to speculate that this shorter disease duration is a consequence of the higher retained dismutation activity in the G93A-39 line, we cannot firmly conclude this.

A transgenic rat model of human ALS will offer several advantages with respect to the existing transgenic mouse ALS models.[15,21] Given its larger size, it will facilitate all studies that entail CSF analysis and, in particular, those that entail multiple, serial manipulations of CSF in the same animal. Thus, it will be possible in this model to obtain adequate CSF for conventional biochemical studies as well as analyzes of small molecules and even DNA/RNA species that may distinguish the ALS from the wild-type CSF. Moreover, this model should be ideal for administration of therapies via chronic intrathecal pumps, a strategy that has been employed recently in human ALS clinical trials.[22] Another advantage of the ALS rats is that they can tolerate some forms of immunosuppressive therapy that are problematic in mice, such as cyclosporine A. This point arises in the context of an emerging interest in possible strategies to use implanted neural stem cells as therapy in ALS. It should now be possible to achieve appropriate immunosuppression in the ALS rats to allow survival of implanted cells and hence determine the efficacy of this approach. As a corollary, we also note that the larger size of the rat spinal cord will facilitate delivery of cells to the target spinal cord regions.

CONCLUSIONS

We have established lines of rats that express transgenes for mutant SOD1 protein with two different ALS-associated mutations: H46R and G93A. As in the human disease and transgenic ALS mice, pathological analysis demonstrates selective loss of motor neurons in the spinal cords of these transgenic rats. In addition, typical neuronal LBHI as well as Ast-HI identical to those in human familial ALS are observed in the spinal cords of the rats. Therefore, at present, we think that the H46R and G93A transgenic rats are neuropathologically most optimal as animal models of familial ALS with the *SOD1*-mutations.

ACKNOWLEDGMENTS

This work was supported by Grant-in-Aid from the Ministry of Health, Labour and Welfare (MA, SK, YI) and Haruki ALS Research Foundation (MA, YI).

REFERENCES

1. Brown RH Jr. Superoxide dismutase in familial amyotrophic lateral sclerosis models for gain of function. *Curr Opin Neurobiol* 1995; **5**: 841–846.
2. Aoki M, Ogasawara M, Matsubara Y *et al.* Mild ALS in Japan associated with novel SOD mutation. *Nat Genet* 1993; **5**: 323–324.

3. Rosen DR, Siddique T, Patterson D *et al.* Mutations in Cu/Zn superoxide dismutase gene are associated with familial amyotrophic lateral sclerosis. *Nature* 1993; **362**: 59–62.
4. Andersen PM, Sims KB, Xin WW *et al.* Sixteen novel mutations in the Cu/Zn superoxide dismutase gene in amyotrophic lateral sclerosis: a decade of discoveries, defects and disputes. *Amyotroph Lateral Scler Other Motor Neuron Disord* 2003; **4**: 62–73.
5. Aoki M, Abe K, Houi K *et al.* Variance of age at onset in a Japanese family with amyotrophic lateral sclerosis associated with a novel Cu/Zn superoxide dismutase mutation. *Ann Neurol* 1995; **37**: 676–679.
6. Deng HX, Tainer JA, Mitsumoto H *et al.* Two novel SOD1 mutations in patients with familial amyotrophic lateral sclerosis. *Hum Mol Genet* 1995; **4**: 1113–1116.
7. Aoki M, Ogasawara M, Matsubara Y *et al.* Familial amyotrophic lateral sclerosis (ALS) in Japan associated with H46R mutation in Cu/Zn superoxide dismutase gene: a possible new subtype of familial ALS. *J Neurol Sci* 1994; **126**: 77–83.
8. Aoki M, Abe K, Itoyama Y. Molecular analyses of the Cu/Zn superoxide dismutase gene in patients with familial amyotrophic lateral sclerosis (ALS) in Japan. *Cell Mol Neurobiol* 1998; **18**: 639–647.
9. Gurney ME, Pu H, Chiu AY *et al.* Motor neuron degeneration in mice that express a human Cu,Zn superoxide dismutase mutation. *Science* 1994; **264**: 1772–1775.
10. Wong PC, Pardo CA, Borchelt DR *et al.* An adverse property of a familial ALS-linked SOD1 mutation causes motor neuron disease characterized by vacuolar degeneration of mitochondria. *Neuron* 1995; **14**: 1105–1116.
11. Bruijn LI, Becher MW, Lee MK *et al.* ALS-linked SOD1 mutant G85R mediates damage to astrocytes and promotes rapidly progressive disease with SOD1-containing inclusions. *Neuron* 1997; **18**: 327–338.
12. Wang J, Xu G, Gonzales V *et al.* Fibrillar inclusions and motor neuron degeneration in transgenic mice expressing superoxide dismutase 1 with a disrupted copper-binding site. *Neurobiol Dis* 2002; **10**: 128–138.
13. Li M, Ona VO, Guegan C *et al.* Functional role of caspase-1 and caspase-3 in an ALS transgenic mouse model. *Science* 2000; **288**: 335–339.
14. Gurney ME, Tomasselli AG, Heinrikson RL. Stay the executioner's hand. *Science* 2000; **288**: 283–284.
15. Nagai M, Aoki M, Miyoshi I *et al.* Rats expressing human cytosolic copper-zinc superoxide dismutase transgenes with amyotrophic lateral sclerosis: associated mutations develop motor neuron disease. *J Neurosci* 2001; **21**: 9246–9254.
16. Cudkowicz M, McKenna-Yasek D, Sapp P *et al.* Epidemiology of SOD1mutations in amyotrophic lateral sclerosis. *Ann Neurol* 1997; **41**: 210–212.
17. Kato S, Shaw P, Wood-Allum C, Leigh PN, Show C. Amyotrophic lateral sclerosis. In: Dickson D (ed.) *Nerodegeneration: the Molecular Pathology of Dementia and Movement Disorders*. Basel: ISN Neuropath Press, 2003; 350–368.
18. Kato S, Saeki Y, Aoki M *et al.* Histological evidence of redox system breakdown caused by superoxide dismutase 1 (SOD1) aggregation is common to SOD1-mutated motor neurons in humans and animal models. *Acta Neuropathol* 2004; **107**: 149–158.
19. Kato S, Saito M, Hirano A, Ohama E. Recent advances in research on neuropathological aspects of familial amyotrophic lateral sclerosis with superoxide dismutase 1 gene mutations: neuronal Lewy body-like hyaline inclusions and astrocytic hyaline inclusions. *Histol Histopathol* 1999; **14**: 973–989.
20. Kato S, Takikawa M, Nakashima K *et al.* New consensus research on neuropathological aspects of familial amyotrophic lateral sclerosis with superoxide dismutase 1 (SOD1) gene mutations: inclusions containing SOD1 in neurons and astrocytes. *Amyotroph Lateral Scler Other Motor Neuron Disord* 2000; **1**: 163–184.
21. Howland DS, Liu J, She Y *et al.* Focal loss of the glutamate transporter EAAT2 in a transgenic rat model of SOD1 mutant-mediated amyotrophic lateral sclerosis (ALS). *Proc Natl Acad Sci USA* 2002; **99**: 1604–1609.
22. Mitsumoto H, Gordon P, Kaufmann P, Gooch CL, Przedborski S, Rowland LP. Randomized control trials in ALS: lessons learned. *Amyotroph Lateral Scler Other Motor Neuron Disord* 2004; **5** (Suppl. 1): 8–13.

Journal of Neuroscience Research 82:63–70 (2005)

Motoneuron Degeneration After Facial Nerve Avulsion Is Exacerbated in Presymptomatic Transgenic Rats Expressing Human Mutant Cu/Zn Superoxide Dismutase

Ken Ikeda,[1,2] Masashi Aoki,[3] Yoko Kawazoe,[1] Tsuyoshi Sakamoto,[1] Yuichi Hayashi,[1] Aya Ishigaki,[3] Makiko Nagai,[3] Rieko Kamii,[3] Shinsuke Kato,[4] Yasuto Itoyama,[3] and Kazuhiko Watabe[1]*

[1]Department of Molecular Neuropathology, Tokyo Metropolitan Institute for Neuroscience, Tokyo, Japan
[2]Department of Neurology, PL Tokyo Health Care Center, Tokyo, Japan
[3]Department of Neurology, Tohoku University Graduate School of Medicine, Sendai, Japan
[4]Department of Neuropathology, Institute of Neurological Sciences, Faculty of Medicine, Tottori University, Yonago, Japan

We investigated motoneuron degeneration after proximal nerve injury in presymptomatic transgenic (tg) rats expressing human mutant Cu/Zn superoxide dismutase (SOD1). The right facial nerves of presymptomatic tg rats expressing human H46R or G93A SOD1 and their non-tg littermates were avulsed, and facial nuclei were examined at 2 weeks postoperation. Nissl-stained cell counts revealed that facial motoneuron loss after avulsion was exacerbated in H46R- and G93A-tg rats compared with their non-tg littermates. The loss of motoneurons in G93A-tg rats after avulsion was significantly greater than that in H46R-tg rats. Intense cytoplasmic immunolabeling for SOD1 in injured motoneurons after avulsion was demonstrated in H46R- and G93A-tg rats but not in their littermates. Facial axotomy did not induce significant motoneuron loss nor enhance SOD1 immunoreactivity in these tg rats and non-tg littermates at 2 weeks postoperation, although both axotomy and avulsion elicited intense immunolabeling for activating transcription factor-3, phosphorylated c-Jun, and phosphorylated heat shock protein 27 in injured motoneurons of all these animals. The present data indicate the increased vulnerability of injured motoneurons after avulsion in the presymptomatic mutant SOD1-tg rats.

Key words: axotomy; facial nerve; amyotrophic lateral sclerosis; ALS; mutant Cu/Zn superoxide dismutase; SOD1; transgenic rat

Since the discovery of the mutation of Cu/Zn superoxide dismutase (SOD1) in patients with familial amyotrophic lateral sclerosis (ALS) and the development of transgenic (tg) mice and rats expressing human mutant SOD1 that show clinicopathological characteristics comparable to human familial ALS, the mutant SOD1-tg animals have been the most widely used experimental models for elucidating the pathomechanism of and the therapeutic approach for familial ALS as well as sporadic ALS (Cleveland and Rothstein, 2001). Although the precise mechanism of motoneuron degeneration in mutant SOD1-tg animals is largely unknown, the mutant SOD1 is thought to have a gain of toxic function (Cleveland and Rothstein, 2001). In another animal model of motoneuron degeneration, peripheral nerve avulsion exhibits extensive loss of motoneurons in adult rats (Søreide, 1981; Wu, 1993; Koliatsos et al., 1994; Watabe et al., 2000; Sakamoto et al., 2000, 2003a,b; Ikeda et al., 2003; Moran and Graeber, 2004). The mechanism of motoneuron degeneration after avulsion also remains unclear, but peroxinitrite-mediated oxidative damage and perikaryal accumulation of phosphorylated neurofilaments have been demonstrated in injured motoneurons after avulsion (Martin et al., 1999). Both of these pathological features have also been shown in

Contract grant sponsor: Ministry of Education, Culture, Sports, Science and Technology, Japan; Contract grant sponsor: Research on Specific Diseases, Health Sciences Research Grants, Ministry of Health, Labor and Welfare, Japan; Contract grant sponsor: Research on Psychiatric and Neurological Diseases and Mental Health, H16-kokoro-017, Ministry of Health, Labor and Welfare, Japan.

*Correspondence to: Kazuhiko Watabe, MD, PhD, Department of Molecular Neuropathology, Tokyo Metropolitan Institute for Neuroscience, 2-6 Musashidai, Fuchu, Tokyo 183-8526, Japan.
E-mail: kazwtb@tmin.ac.jp

Received 6 April 2005; Revised 31 May 2005; Accepted 30 June 2005

Published online 17 August 2005 in Wiley InterScience (www.interscience.wiley.com). DOI: 10.1002/jnr.20621

spinal motoneurons in mutant SOD1-tg animals as well as in patients with familial and sporadic ALS (Estévez et al., 1998; Cleveland, 1999; Cleveland and Rothstein, 2001). If motoneuron degeneration after peripheral nerve avulsion shares any underlying mechanisms of motoneuron death associated with SOD1 mutation, motoneurons in presymptomatic mutant SOD1-tg animals may be more susceptible to pathological insults following avulsion compared with their non-tg littermates. If this is so, we may be able to utilize facial nerve avulsion as an animal model for understanding the mechanisms of motoneuron degeneration in ALS. In the present study, we examined injured motoneurons after facial nerve avulsion in presymptomatic mutant human SOD1-tg rats and their littermates.

MATERIALS AND METHODS

Animals and Surgical Procedures

The experimental protocols were approved by the Institutional Animal Care and Use Committee of Tokyo Metropolitan Institute for Neuroscience and Tohoku University Graduate School of Medicine. The tg rats expressing human mutant SOD1 (H46R, G93A) were generated as described previously (Nagai et al., 2001). Two types of rats with SOD1 mutations, H46R and G93A, were used for experiments. The H46R-tg rats develop motor deficits at about 140 days of age and die after 3 weeks, and G93A-tg rats show the clinical signs at around 120 days of age and die after 10 days (Nagai et al., 2001).

The presymptomatic female H46R (90 days old)- and G93A (80 days old)-tg rats were anesthetized with inhalation of halothane. Under a dissecting microscope, the right facial nerve was exposed at its exit from the stylomastoid foramen. With microhemostat forceps, the proximal facial nerve was avulsed by gentle traction and removed from the distal facial nerve as described elsewhere (Sakamoto et al., 2000, 2003a,b; Ikeda et al., 2003). As for axotomy, the right facial nerve was transected at its exit from the stylomastoid foramen, and a distal portion of the nerve, 5 mm in length, was cut and removed. The wound was covered with a small piece of gelatin sponge (Gelfoam; Pharmacia Upjohn, Bridgewater, NJ) and closed by fine suture.

Motoneuron Cell Counting

At 2 weeks postoperation, rats were anesthetized with a lethal dose of pentobarbital sodium and transcardially perfused with 0.1 M phosphate buffer, pH 7.4 (PB), followed by 4% paraformaldehyde in 0.1 M PB. The brainstem tissue was excised, postfixed in the same fixative for 2 hr, dehydrated, and embedded in paraffin, and serial transverse sections (6-μm thickness) were made. Every fifth section (24-μm interval) was collected, deparaffinized, and stained with cresyl violet (Nissl staining), and facial motoneurons having nuclei containing distinct nucleoli on both sides of the facial nuclei were counted in 25 sections as described elsewhere (Sakamoto et al., 2000, 2003a,b; Ikeda et al., 2003). The data were expressed as the mean ± SEM, and statistical significance was assessed by Mann-Whitney U-test.

Immunohistochemistry

Immunohistochemistry on paraffin sections was performed with the following primary antibodies: sheep anti-human SOD1 (1:1,000; Calbiochem, San Diego, CA), rabbit anti-human SOD1 (1:10,000; kindly provided by Dr. K. Asayama; Asayama and Burr, 1984), mouse monoclonal anti-phosphorylated neurofilament SMI-31 (1:1,000; Sternberger Monoclonals, Lutherville, MD), rabbit anti-ubiquitin (1:1,000; Dako, Glostrup, Denmark), rabbit anti-glial fibrillary acidic protein (GFAP; 1:1,000; Dako), rabbit anti-activating transcription factor-3 (ATF3; sc-188, 1:200; Santa Cruz Biotechnology, Santa Cruz, CA), rabbit anti-c-Jun (sc-1694, 1:200; Santa Cruz Biotechnology), mouse monoclonal anti-phosphorylated c-Jun (sc-822, 1:200; Santa Cruz Biotechnology), rabbit anti-heat shock protein (Hsp) 25 that reacts with rat Hsp27 (SPA-801, 1:200; Stressgen, Victoria, British Columbia, Canada), and rabbit anti-phosphospecific (Ser^{15})Hsp27 (1:200; Oncogene, San Diego, CA). For immunohistochemistry, deparaffinized sections were pretreated with 0.3% H_2O_2 in methanol and preincubated with 3% heat-inactivated goat or rabbit serum in 0.1% Triton X-100 in phosphate-buffered saline (T-PBS). In cases of immunostaining with mouse primary antibodies, MOM blocking kit (Vector, Burlingame, CA) was used according to the manufacturer's instructions to reduce nonspecific background staining. Sections were then incubated overnight at 4°C with the primary antibodies diluted in T-PBS, followed by the incubation with biotinylated rabbit anti-sheep, goat anti-rabbit, or goat anti-mouse IgG at a dilution of 1:200 and with ABC reagent (Vector), visualized by 3,3′-diaminobenzidine tetrahydrocholoride (DAB)-H_2O_2 solution and counterstained with hematoxylin. For negative controls, the primary antibodies were omitted or replaced by nonimmunized animal sera.

RESULTS

Two weeks after avulsion of the right facial nerves in non-tg littermates, the number of surviving facial motoneurons declined to ~70% of that on the contralateral side, similar to that in normal rats, as described previously (Sakamoto et al., 2000). In SOD1-tg rats, only ~30–50% of motoneurons survived 2 weeks after avulsion, indicating that the loss of motoneurons was exacerbated in SOD1-tg rats compared with their non-tg littermates (Fig. 1, Table I). The numbers of surviving motoneurons in G93A-tg rats after avulsion (~35% of contralateral side) were significantly less than those in H46R-tg rats (~50% of contralateral side; Table I). The numbers of intact motoneurons at contralateral sides did not differ between tg rats and non-tg littermates, indicating that cell loss does not happen at this moment in the course of the disease with SOD1 mutations (Table I). Facial nerve axotomy did not induce significant loss of injured motoneurons in tg rats and non-tg littermates at 2 weeks postoperation (Fig. 1, Table I).

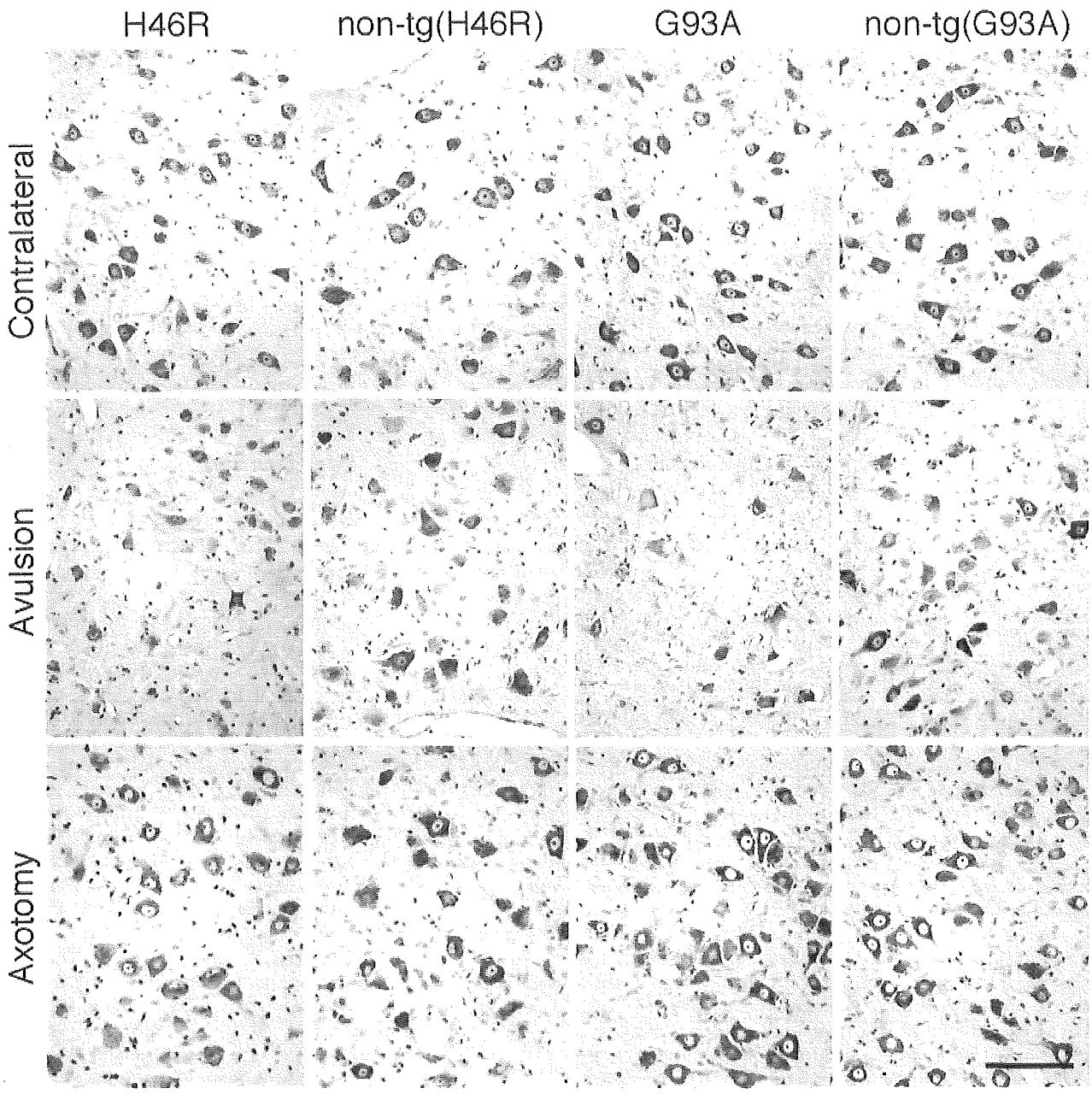

Fig. 1. Facial motoneurons of H46R- and G93A-transgenic (tg) rats and their non-tg littermates on the contralateral and ipsilateral (avulsion or axotomy) sides 2 weeks after facial nerve avulsion or axotomy. Nissl stain. Scale bar = 100 μm.

Examination of sections immunostained for SOD1 showed intense cytoplasmic immunolabeling for SOD1 in injured motoneurons after avulsion in H46R- and G93A-tg rats compared with uninjured motoneurons on the contralateral side that were not or were very faintly immunoreactive for SOD1 (Fig. 2). We used sheep and rabbit anti-SOD1 antibodies, both of which gave identical results. The cytoplasmic SOD1 immunolabeling patterns of injured motoneurons appeared diffuse in H46R-tg rats, whereas they were granular in G93A-tg rats. In G93A-tg rats, there were axons and vacuolar changes in the neuropil consistently immunoreactive for SOD1 at both uninjured and injured sides of facial nuclei (Fig. 2). There was no definite immunolabeling for SOD1 in either injured or uninjured motoneurons and their axons in non-tg littermates (Fig. 2). Facial nerve axotomy did not increase immunoreactivity for SOD1 in injured motoneurons of tg rats and non-tg littermates at 2 weeks

TABLE I. Survival of Motoneurons After Facial Nerve Avulsion and Axotomy[†]

Rat (n)	Ipsilateral motoneuron number	Contralateral motoneuron number	Survival %
Avulsion			
NL (H46R) (n = 10)	598 ± 18	813 ± 26	73.7 ± 1.2
H46R (n = 8)	402 ± 36*	839 ± 27	47.5 ± 2.8*
NL (G93A) (n = 6)	637 ± 56	822 ± 47	76.7 ± 3.0
G93A (n = 7)	306 ± 37*	884 ± 44	34.7 ± 3.6*,**
Axotomy			
H46R (n = 5)	751 ± 19	843 ± 23	89.2 ± 1.4
NL (G93A) (n = 6)	743 ± 15	835 ± 12	88.9 ± 0.6
G93A (n = 5)	741 ± 42	781 ± 45	94.9 ± 1.2

[†]Numbers of facial motoneurons and the percent survival at the ipsilateral (lesion) side relative to the contralateral (control) side 2 weeks after avulsion or axotomy. Results are presented as mean ± SEM. Statistical comparison was done by Mann-Whitney U-test. n = number of animals. NL, nontransgenic littermates.
*$P < 0.01$ vs. NL (H46R) and NL (G93A) rats after avulsion.
**$P < 0.05$ vs. H46R-transgenic rats after avulsion.

postoperation (Fig. 2). In contrast, immunohistochemical examination showed perikaryal accumulation of phosphorylated neurofilaments in injured motoneurons both after axotomy and after avulsion, as described previously (Koliatsos et al., 1989, 1994; Koliatsos and Price, 1996). There were no hyaline inclusions identifiable in HE-stained sections or ubiquitin-immunoreactive structures in both H46R- and G93A-tg rats and their non-tg littermates on either operated or contralateral sides (data not shown). Proliferation of astrocytes as evidenced by immunostaining for GFAP was observed at the injured sides in all the animals after avulsion and axotomy, and the degree of the astrocytic response appeared to correlate with the extent of motoneuron loss after avulsion; i.e., more intense GFAP immunostaining was demonstrated when less neuronal survival was observed (Fig. 3).

It has been shown that ATF3 is expressed, and c-Jun and Hsp27 are up-regulated and phosphorylated, in injured motoneurons after axotomy (Tsujino et al., 2000; Casanovas et al., 2001; Benn et al., 2002; Kalmár et al., 2002). Several reports have documented that ATF3, c-Jun, and Hsp27 cooperate to promote neuronal survival in vitro and in vivo, suggesting neuroprotective roles of these molecules (Pearson et al., 2003; Nakagomi et al., 2003). We then examined the expression of ATF3, c-Jun, and Hsp27 in injured motoneurons after facial nerve avulsion that causes extensive neuronal loss. In wild-type adult rats, intact facial motoneurons were constitutively immunoreactive for c-Jun and Hsp27 but not for ATF3, phosphorylated c-Jun, or phosphorylated Hsp27, whereas injured motoneurons become immunoreactive for ATF3, phosphorylated c-Jun, and phosphorylated Hsp27 within 1 day after facial nerve avulsion and remain positive up to 4 weeks (Watabe et al., unpublished observations). In a similar manner, virtually all injured motoneurons were immunostained for ATF3, phosphorylated c-Jun, and phosphorylated Hsp27 in H46R- and G93A-tg rats and their non-tg littermates 2 weeks after avulsion and axotomy as examined in this study (Fig. 3).

DISCUSSION

We demonstrated that only 50% (H46R-tg rats) or 35% (G93A-tg rats) of motoneurons in mutant SOD1-tg rats survived 2 weeks after avulsion at their presymptomatic stage compared with 70% survival of motoneurons in their non-tg littermates, indicating that motoneuron degeneration after avulsion is significantly more severe in these presymptomatic mutant SOD1-tg rats. It is interesting to note that the loss of motoneurons in G93A-tg rats was significantly greater than that in H46R-tg rats after avulsion, insofar as the onset of paralysis is earlier and the disease progression is more rapid in G93A-tg rats compared with the H46R rats used in the present study (Nagai et al., 2001). The clinical courses of these tg rats are also likely to be relevant to those of human mutant SOD1-mediated familial ALS, in that the human H46R cases progress very slowly compared with the G93A cases (Nagai et al., 2001; Aoki et al., 1993, 1994). In contrast, we did not see significant motoneuron loss in the presymptomatic SOD1-tg rats and their non-tg littermates 2 weeks after facial nerve axotomy. Unlike avulsion, axotomy does not generally induce significant motoneuron death in adult rodents (Lowrie and Vrbová, 1992; Moran and Graeber, 2004), except that, in the case of adult Balb/C mice, the facial nerve axotomy leads to loss of >50% of the motoneurons at 30 days postoperation (Hottinger et al., 2000), and C57BL mice show late motoneuron loss (~60%) 8 weeks after facial nerve axotomy (Angelov et al., 2003). Mariotti et al. (2002) axotomized facial nerves of G93A-tg mice and their non-tg littermates at their presymptomatic stage and observed loss of facial motoneurons that was higher in G93A-tg mice than in non-tg littermates at 30 days postaxotomy; these data are relevant to our present data acquired from avulsion, but not axotomy, in rats, which probably is due to the use of different animal species. In contrast, Kong and Xu (1999) described axotomy of lumbar spinal or sciatic nerve in G93A-tg mice at the presymptomatic stage reducing the extent of axon degeneration at the end stage of the disease. They did

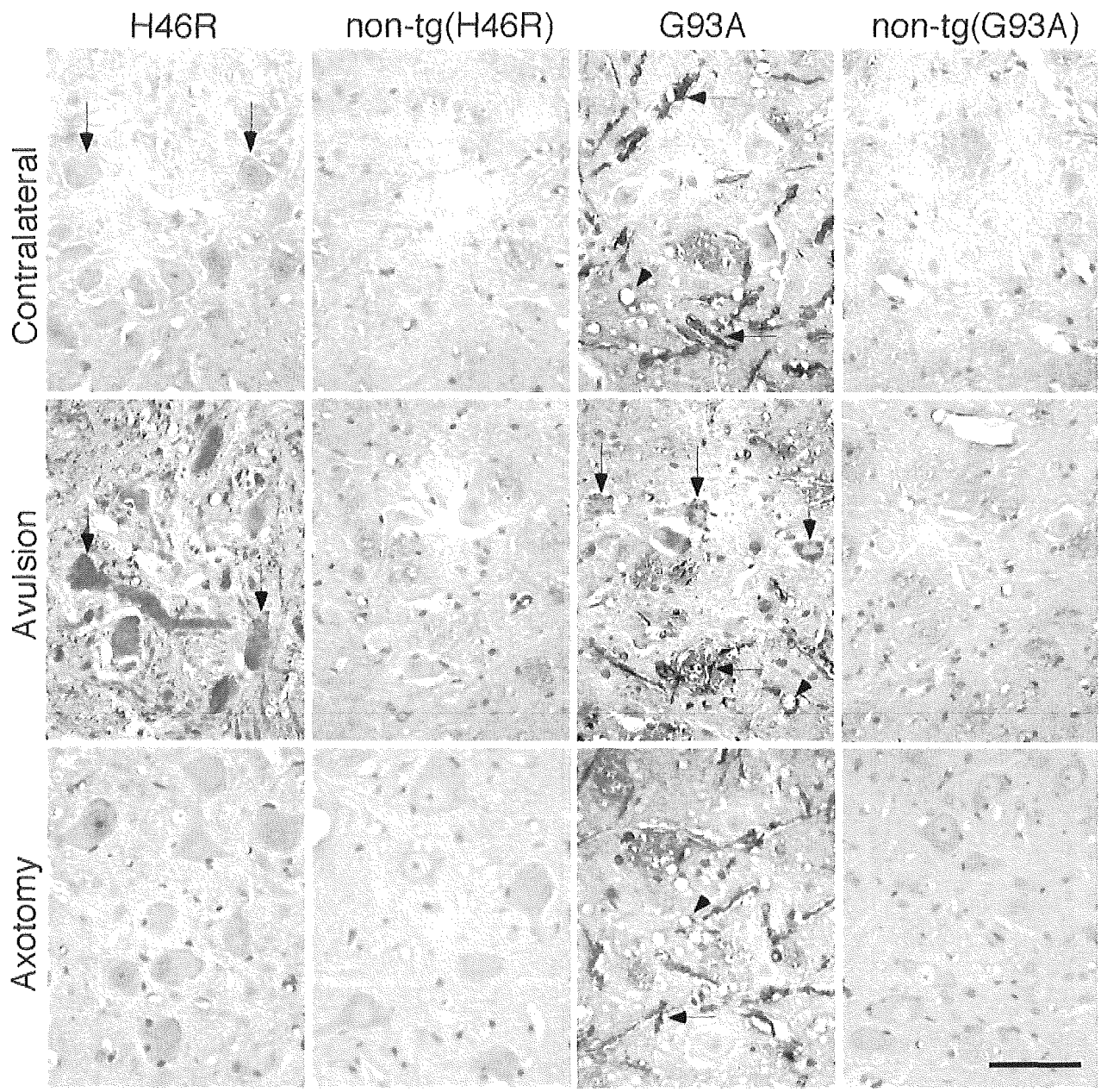

Fig. 2. SOD1 immunohistochemistry of facial motoneurons of H46R- and G93A-tg rats and their non-tg littermates on the contralateral and ipsilateral (avulsion or axotomy) sides 2 weeks after facial nerve avulsion or axotomy. Counterstained with hematoxylin. Note immunostained motoneurons (vertical arrows), axons (horizontal arrows), and vacuoles in neuropil (arrowheads) in H46R- and G93A-tg rats. Scale bar = 50 μm.

not evaluate the response of the cell bodies of spinal motoneurons, so it remains unknown whether SOD1 mutation affects the viability of spinal motoneurons after axotomy. In the present study, we demonstrated that motoneuron degeneration after facial nerve avulsion, but not after axotomy, is exacerbated in presymptomatic mutant SOD1-tg rats at 2 weeks postoperation. These data clearly indicate the increased vulnerability of facial motoneurons to proximal nerve injury in the presymptomatic SOD1-tg rats.

It has been shown that SOD1 is abundantly expressed in cell bodies, dendrites, and axons of wild-type mouse and rat motoneurons in vivo (Pardo et al., 1995; Moreno et al., 1997; Yu, 2002). In the present